

UNCLASSIFIED

DEPARTMENT OF DEFENCE

AR-001-893

DEFENCE SCIENCE AND TECHNOLOGY ORGANISATION

ELECTRONICS RESEARCH LABORATORY

TECHNICAL REPORT

ERL-0099-TR

RADIOMETRIC MEASUREMENTS USING LINE SCANNED  
INFRARED IMAGING SYSTEMS

G.V. Poropat

S U M M A R Y

The use of line scanned imaging systems in performing radiometric measurements enables the collection of considerable amounts of data which may be used in determining the distribution of radiant energy from a source. The interpretation of this data may be subject to errors due to the detector field of view and the scanning process. The sources of these errors and their magnitude are considered and guidelines for the analysis of the data developed.

Approved for Public Release

---

POSTAL ADDRESS: Chief Superintendent, Electronics Research Laboratory,  
Box 2151, G.P.O., Adelaide, South Australia, 5001.

---

UNCLASSIFIED

## TABLE OF CONTENTS

	Page No.
1. INTRODUCTION	1
2. SOURCES OF ERROR IN RADIOMETRIC DATA	1 - 8
2.1 Errors due to the detector field of view and processing electronics	1 - 6
2.2 Errors due to the sampling of data	6 - 8
3. ERRORS IN REAL DATA	8 - 10
4. ANALYSIS OF DATA	10 - 11
5. CONCLUSION	11
REFERENCES	12

## LIST OF FIGURES

1. Signal flow graph for data acquisition and analysis
2. AGA Thermovision line spread function
3. Pulse transfer function obtained using a gaussian line spread function
4. Pulse correction factor as a function of pulse width
5. Variation of integral error with integration limits

## 1. INTRODUCTION

The measurement of the radiant energy emitted from bodies has traditionally been performed with radiometers which have a fixed field of view and often a fixed orientation. The determination of the amount of infrared radiation emitted from bodies of complex shape, with complex distribution of radiance over this surface or against non-uniform or time varying backgrounds involves considerable effort when performed with this type of instrument. The development of scanning radiometers and in particular imaging systems operating in the infrared region of the electromagnetic spectrum has facilitated such measurement since the scanning radiometer signals provide a mapping of the spatial radiance distribution into the time domain. The amount of data which can be gathered with the use of this form of instrument is considerably greater than that which could be obtained with a fixed radiometer. However care must be taken in the interpretation of these data if the effects of the scanning process are not to introduce significant errors in the interpretation of the data.

Night Vision Group uses an AGA Thermovision as part of its infrared instrumentation. To facilitate the analysis of data obtained a system for image recording and storage has been developed(ref.1). This stores the image in digital form, thus necessitating sampling of the AGA video signal. When interpreting data obtained from the AGA Thermovision the effects of the sampling process must be accounted for in any analysis. Further, since the AGA Thermovision is an imaging instrument the raster structure of the picture introduces a sampling in the vertical direction, which will also effect interpretation of the data.

This report discusses aspects of the data acquisition and analysis using this equipment which can introduce errors into the results obtained. The effect of the limited detector resolution on the video data from point sources has been determined for the AGA Thermovision used by Night Vision Group and the analysis has been extended to the accuracy of estimates of emission from extended non-uniform sources. The analysis of the sources of error leads to the conclusion that for extended sources whose radiance distributions have no significant components at very high spatial frequencies the use of an instrument such as the AGA Thermovision in obtaining data is not subject to significant errors, however for small sources and extended sources with significant detail careful interpretation of any data must be made if the errors in determination of radiometric data are not to become significant.

## 2. SOURCES OF ERROR IN RADIOMETRIC DATA

Figure 1 illustrates the signal flow graph for data acquisition and analysis using the AGA Thermovision and shows the major 'noise' sources, which may be considered as error sources.

In the analysis of the sources of error we will consider errors due to the line by line sampling of the scanning process and the sampling of data for image formation and storage. Errors may be introduced by any electronics in the system due to non linearities and noise in the electronics but these will not be considered here, the effect of limited bandwidth in the electronics will however be considered.

### 2.1 Errors due to the detector field of view and processing electronics

For both fixed and scanning radiometers the effect of the instantaneous field of view on the data obtained must be considered. In the case of the scanning instrument this field of view is moved across the target distribution and transforms the observed radiance distribution into a time varying voltage through the mechanism of the detector's response to the radiation incident on it. The instantaneous field of view of the instrument is modified by aberrations in the optical system and can have a non-uniform response across its extent. In general the detector size determines the

main properties of the point spread function of an imaging instrument through the size of the instantaneous field of view.

The observed signal, at any point  $(x,y)$  on a two dimensional distribution, produced by a radiometer is given by

$$v(x,y) = \int_{-\infty}^{\infty} \int_{-\infty}^{\infty} N(x^1, y^1) g(x-x^1, y-y^1) dx^1 dy^1$$

where  $N(x,y)$  is the effective radiance distribution in the  $x,y$  plane and  $g(x,y)$  is the point spread function of the system. If the target distribution  $N(x,y)$  is of greater extent than the point spread function and if  $N(x,y)$  is uniform the observed signal will be uniform and proportional to  $N(x,y)$ , however if  $N(x,y)$  is of an extent of the order of  $g(x,y)$  or smaller, then the observed signal  $v(x,y)$  is no longer directly proportional to  $N(x,y)$ . In effect the observed amplitude of any target radiance distribution is decreased if that distribution is of spatial extent of the order of or less than the point spread function.

In measuring radiometric data we often wish to determine the instantaneous value of the function  $N(x,y)$  and the total emission from a given

area which is given by  $\iint_S N(x,y) dx dy$  where  $S$  is the area of interest,

both these quantities are effected by the relationship between the radiance distribution and the point spread function used to scan it.

In order to estimate the errors involved in obtaining the peak signal from a uniform distribution of finite extent we will consider the one dimensional scanning process. The uniform radiance distribution can be considered as a rectangular pulse function and if  $g(t)$  is the one dimensional point spread function (line spread function) the observed signal from a one dimensional scanning sequence of infinite length is

$$v(t) = \int_{-\infty}^{\infty} p(a) g(t-a) da$$

where  $p(a)$  is the pulse input.

If the integration limits are put equal to the scan dimensions of the instrument the observed signal will not differ from this significantly unless the line spread function is significant in extent with respect to these integration limits i.e. the resolution is of the order of the field of view.

The line spread function of the AGA Thermovision currently used by Night Vision Group has been measured and is shown in figure 2 with the modulation transfer function calculated for a symmetrical Gaussian line spread function. The line spread function can be approximated by the gaussian function,

$e^{-\beta t^2}$  (where  $\beta = 2.56 \times 10^{10}$ ) as shown in figure 2 to ease computational

difficulties. If the pulse function  $p(a)$  is defined as  $p(a) = 1$ ,  $-t_1 < a < +t_1$  and  $p(a) = 0$  elsewhere then using the gaussian approximation to the line spread function the observed signal is

$$\begin{aligned}
 v(t) &= \int_{-\infty}^{\infty} p(a) e^{-\beta(t-a)^2} da \\
 &= \int_{-t_1}^{+t_1} e^{-\beta(t-a)^2} da \\
 &= \int_{\sqrt{\beta}(-t_1-t)}^{\sqrt{\beta}(t_1-t)} \frac{1}{\sqrt{\beta}} e^{-x^2} dx \\
 &= \frac{1}{\sqrt{\beta}} \left[ \int_0^{\sqrt{\beta}(t_1-t)} e^{-x^2} dx - \int_0^{\sqrt{\beta}(t_1+t)} e^{-x^2} dx \right] \\
 &= \frac{\sqrt{\pi}}{2\sqrt{\beta}} [\operatorname{erf}(\sqrt{\beta}(t_1-t)) + \operatorname{erf}(\sqrt{\beta}(t_1+t))] \quad (1)
 \end{aligned}$$

and this function is plotted in figure 3 for varying values of  $t_1$  (pulse width) for  $\beta = 2.56 \times 10^{10}$ .

It can readily be seen that as the slit width decreases the peak signal observed for constant amplitude input decreases, falling to 50% when the product  $\sqrt{\beta} \cdot t_1$  is .475. For slit widths ( $2t_1$ ) of three times the effective gaussian line width the peak signal amplitude observed is not subject to significant errors.

For the AGA Thermovision in use this corresponds to a target extent of 6 mrad. The field view of the AGA is 70 mrad and thus considerable care must be exercised in these measurements. Figure 4 shows the correction factor to be applied to the observed signal amplitude for various target extents.

The total emission from a target is given by the integral of the radiance distribution over the extent of the target and this is

$$V = \iint_S N(x,y) dx dy$$

where  $S$  is the surface defining the extent of the target.

The emission measured by the AGA Thermovision is:

$$V^1 = \iint_S N(x,y) * g(x,y) dx dy$$

where \* is the convolution operator and  $g(x,y)$  is the point spread function. The error in the measured emission is

$$V - V^1 = \iint_S N(x,y) dx dy - \iint_S N(x,y) * g(x,y) dx dy.$$

If we extend the integration limits to infinity and assume no emission from the background

$$\begin{aligned} V - V^1 &= \iint_{-\infty}^{\infty} N(x,y) dx dy - \iint_{-\infty}^{\infty} N(x,y) * g(x,y) dx dy \\ &= \iint_{-\infty}^{\infty} N(x,y) e^{j\omega_x x} e^{j\omega_y y} dx dy \\ &\quad - \iint_{-\infty}^{\infty} N(x,y) * g(x,y) e^{j\omega_x x} e^{j\omega_y y} dx dy \end{aligned}$$

$$\text{for } \omega_x = 0 \text{ and } \omega_y = 0$$

$$= N_{Txy}(0) - N_{Txy}(0) \cdot g_{Txy}(0)$$

where  $N_{Txy}(0)$  is the two dimensional Fourier Transform evaluated at  $\omega_x$  and  $\omega_y = 0$  (i.e. the D.C. component of  $N(x,y)$ ) and  $g_{Txy}(0)$  is the two dimensional Fourier Transform of  $g(x,y)$ .

The percentage error is then

$$E = (1 - g_{Txy}(0)) \cdot 100$$

For a perfect system with a  $\delta$ -function output as its impulse response,  $g_{Txy}(0) = 1$ , and the percentage error is zero.

For such a system, the steady state response to a unit step function input is an output signal of unity amplitude. In order to compare systems we will impose the requirement that the systems produce a steady state response of unity amplitude when driven by a unit step input.

The output of such a system for a unit step input at zero time is

$$h(t) = \int_0^{\infty} g(t-x) dx$$

where  $g(t)$  is the system impulse response.

Changing the variable of integration

$$h(t) = \int_{-\infty}^t g(x) dx$$

and the steady state response is

$$h(\infty) = \int_{-\infty}^{\infty} g(x) dx = g_{Txy}(0) = 1$$

For integration over all time for any system of this kind then the percentage error in the estimate of total energy emitted is zero. However in any real time system the integration does not extend over all time but is limited to a finite range. The estimation of the percentage error in this case involves a knowledge of  $N(x,y)$  and  $g(x,y)$  and the evaluation of the integrals involved.

Obviously  $N(x,y)$  is not known and therefore error estimates can only be approximate without resort to complex analysis which may obtain  $N(x,y)$ . To obtain an estimate of the error we can again consider the response of an imaging system with gaussian line spread function to a rectangular pulse input.

Referring to equation (1) the response of a system with gaussian line spread function to a rectangular pulse is

$$V(t) = \frac{\sqrt{\pi}}{2\sqrt{\beta}} (\text{erf}(\sqrt{\beta}(t_1 - t)) + \text{erf}(\sqrt{\beta}(t_1 + t))) \text{ where } \beta \text{ and } t,$$

have their previous meaning. For any given pulse input the integrated system response is obtained by

$$V = \int_{t_1^1}^{t_2^1} v(t) dt$$

where the integration limits are defined by  $t_1^1$  and  $t_2^1$ .

For  $t_1^1$  and  $t_2^1$  very large, numerical integration of the system response produces a result which is not significantly different from the integral of the input signal, a result which is in agreement with the previous argument. However as the range of integration is shortened the result  $V$  differs from the integral of the input signal and the error is found to be a function of the duration of the input pulse, the range of integration limits and the line spread function. For the rectangular pulse shape used the absolute error in the integral estimate for integration limits fixed with respect to the pulse boundaries (i.e. for limits which remain constant with respect to the pulse edges) is constant for pulse widths of sufficient extent that the observed maximum signal reaches the pulse maximum. Figure 5 illustrates the variation in integral error with pulse length and integration limits.

From the results it can be seen that for input signals whose extent is of the order of the line spread function and greater, the integral of the output signal when taken over limits which are half the line spread function greater in extent than the pulse length is such that the error in the

integral is of the order of 2% and decreases with increasing input signal extent. The data being analysed in real cases cannot be related to a known input signal and hence the limits of integration are chosen on the basis of the perceived edge of the target as defined by the observer. Generally this will be the region of greatest slope at the edge which will correspond to integration limits of slightly less than those of the line spread function width and the resulting error will thus be slightly greater, although this will be of the order of five percent for input signals whose extent is that of the line spread function and will again decrease for signals of longer extent.

For input signals whose extent is less than the line spread function width the integration must be performed over the extent of the line spread function or the error will very quickly rise to unacceptable limits as the integration period is truncated.

It is convenient at this point to discuss the errors due to the limited bandwidth in the processing electronics. The scanning process transforms the spatial signal to a temporal signal with the transformation  $x = vt$ , where  $v$  is the scanning velocity of the sensor. For a point source scanned by a detector with a Gaussian point spread function whose output is amplified by a single pole filter of bandwidth  $\omega_0$  the observed output signal is

$$g(t) = \int_{-\infty}^{\infty} \frac{\omega_0}{2} e^{-\beta t^2} e^{-\omega_0 (t - \tau)} d\tau \quad (\text{reference 2})$$

The observed output of the filter has a peak value less than the input to the filter. The gaussian pulse shape of the input is skewed and becomes asymmetrical although the degree to which this occurs is not of great significance. For the estimated 80 kHz bandwidth of the amplifiers used in the AGA Thermovision a decrease of 7% in peak signal value is predicted on the basis of a Gaussian line spread function and a correction factor of this order must therefore be included in any estimate of point source amplitudes with respect to extended sources.

The effect of the filter on the integral of the observed signal will be of the same form as the effect of the line spread function. The effective 3 db bandwidth of the Gaussian line spread function is only 20 kHz and the magnitude of the error in the estimate of the integral introduced by the limited bandwidth of the AGA electronics is considerably less than that due to the line spread function.

These errors are inherent in the use of the AGA Thermovision and therefore must be accounted for in any measurements made with this instrument since without resorting to techniques such as enhancement of the image resolution by inverse filtering of the data no improvement in the resolution of the information is available.

## 2.2 Errors due to the sampling of data

In scanning the field of view over which the AGA Thermovision operates the detector effectively samples the radiance distribution in the field of view along the vertical axis every .9 mrad. The data from the AGA is digitised and stored in a semi-conductor memory and this process involves the sampling of the data in time and thus effectively along the horizontal axis every .9 mrad. The data upon which much of the analysis will be performed then consists of matrix of picture elements representing the two dimensional sampling of the radiance distribution in the field of view. The processing (for example integration of the total signal from a target) which is performed on this data is performed digitally and it is therefore necessary to quantify the sources of error in the processing of this data.

If the data were to be restored to analogue form this is achieved theoretically with a filter having unity gain in the pass band and zero gain



elsewhere. The impulse response of this form of filter is a sinc function and the response obtained is the convolution of this function with the comb-like function representing the sample values. Extrapolation between sample values does not therefore give the correct values for the reconstructed video signal although the errors are only appreciable if the sampling rate is low compared to the Nyquist frequency for a band limited signal.

The sampling rate used in the AGA data acquisition system is 156.25 kHz and this is consistent with a system Modulation Transfer Function of less than 10% at 60 kHz, for acceptable levels of aliasing(ref.2). Step wise reconstruction of the data in effect convolves the sampled data with a rectangular pulse function rather than the sinc function theoretically required for data restoration. The additional error in the integration of data reconstructed in this manner can be expressed as the quantity.

$$e(t) = \int_{t_1}^{t_2} v(t) dt - \sum_{i=0}^{n-1} v(t_1 + i\Delta t) \cdot \Delta t$$

where  $v(t)$  is the video signal under consideration and  $\Delta t$  is the sampling interval(ref.3). The second term in this quantity is a Riemann sum of the form

$$R_n = h \sum_{k=0}^{n-1} f(a + kh)$$

where

$$h = \frac{b-a}{n}.$$

If  $f(t)$  is continuous in the interval  $(t_1, t_2)$  over which the  $n$  samples are obtained then

$$\left| \int_{t_1}^{t_2} f(t) dt - \Delta t \sum_{h=0}^{n-1} f(t_1 + k\Delta t) \right| \leq (t_2 - t_1) w(\Delta t)$$

where  $w(\Delta t)$  is the maximum change in  $f(t)$  in  $\Delta t$  in the interval under consideration. The quantity  $w(\Delta t)$  therefore is the determining factor for a given integration process over a fixed interval. The effect of the finite field of view of the detector used for scanning the field of view is to put a limit on the quantity  $w(\Delta t)$  e.g. a point source produces the point spread function response described previously.

The point source is in effect the worst case input to the system and an estimate of the error involved in evaluating the emission from a point source is of importance. The quantity  $(t_2 - t_1) w(\Delta t)$  represents a maximum upperbound on the error in the integral. For the line spread function integrated from 25  $\mu s$  before its maximum to 25  $\mu s$  after its maximum this upper bound represents an error of approximately 30%. However since  $w(\Delta t)$  has its maximum at only one discrete point on either side of the maximum value of the line spread function this upper bound is considerably in excess of the true error estimate for the line spread function. In practice the observed error will be of the order of 2 to 5%.

For any typical signal not having significant spatial frequency components above 0.25 cycles/mrad (36.6 kHz) the numerical integral given by the Riemann sum can be expected to yield an accuracy of the order of 1 to 2% when the integral is performed over 10 or more sampling periods.

### 3. ERRORS IN REAL DATA

The preceding analyses have in general been concerned with step or impulse functions and in general these are only components of the observed scene. It is therefore necessary to gain some appreciation of the structure of the data on which the analysis is to be performed, and to do this a knowledge of the distribution of the spatial frequency components in the data is necessary and this was obtained by performing an analysis on some real data using the Discrete Fourier Transform.

The spatial frequency distribution of the video data in the horizontal direction can be determined using the data acquisition system and applying a Fast Fourier Transform to the data line-by-line. In a manner analogous to the use of the Modulation Transfer Function Area as a descriptor of picture or imaging system quality we can use the integral of the spectral distribution over the spatial frequency range as a descriptor of information content.

In applying the Fast Fourier Transform to the data it must be remembered that the data sample is restricted in time, the data values are quantised using an 8 bit analogue to digital converter and the number of samples taken per line is not large enough to produce very good resolution in the frequency components. The noise inherent in the data introduces a noise component at every frequency of interest in the range over which the analysis is performed and this results in difficulty in defining a frequency at which information may be considered of importance or otherwise.

The results of applying the F.F.T. to various data and summing the frequency components were found to be, that on average 95 percent of the integrated spectral distribution is found to be below 50 kHz for approximately 50 percent of the data examined. Only 10% of the data examined was found to have a spectral distribution for which 95% of the total did not occur below 60 kHz. These results are obtained from data with significant detail in the field of view and are considered to represent limits which may be applied to average data. These results also include the effects of wide band electronic noise (which contributes to the observed frequency coefficients), quantisation noise from the analogue to digital converter and "smearing" due to windowing of data in applying the F.F.T.

The quantisation of data can add significantly to the signal to noise ratio observed with the calculated F.F.T. coefficients. The F.F.T. is defined as

$$X(k) = \sum_{n=0}^{N-1} x(n) w_N^{kn} \quad k = 0, 1, 2 \dots N-1$$

where the  $x(n)$  are the values of the  $N$  samples used and the  $w_N^{kn}$  are given by

$$w_N^{kn} = \exp(-2\pi i kn/N)$$

The quantisation process in the analogue to digital converter can be described by the addition of a noise component such that

$$x^1(n) = x(n) + \epsilon(n)$$

where  $x^1(n)$  is the analogue to digital converter output,  $x(n)$  is the analogue data value and  $\epsilon(n)$  is the error signal. The term  $\epsilon(n)$  represents a random variable which is evenly distributed over the range  $-0.5 \times 2^{-2b} < \epsilon(n) < +0.5 \times 2^{-2b}$  where  $b$  is the number of bits used in the quantisation and  $\epsilon(n)$  has variance  $\frac{2^{-2b}}{12}$  and mean of zero(ref.4),

The mean square magnitude of the calculated frequency coefficient of the Fast Fourier Transform is (neglecting rounding effects in the arithmetic).

$$\begin{aligned} E((x(k))^2) &= E\left(\sum_{n=0}^{N-1} x^1(n) w_N^{kn}\right) \\ &= N.E((x^1(n))^2) \text{ since the } w_N^{kn} \text{ are orthogonal} \\ &= N.E((x(n))^2) + N.E(\epsilon(n)^2) \text{ where } E(\ ) \text{ is the expectation operator} \\ &= N.\sigma_x^2 + N.\left(\frac{2^{-2b}}{12}\right) \text{ for a zero mean variable } x(n). \end{aligned}$$

Thus the observed signal to noise ratio at the output of the F.F.T. for quantised input data is

$$S/N = \frac{12 \sigma_x^2}{2^{-2b}} \text{ for zero mean data.}$$

For a gaussian noise chosen so that  $\sigma_x = \frac{1}{2}$  (i.e. there is very low probability of the signal exceeding the available dynamic range which is assumed to be unity) for bipolar signals we have for an 8 bit quantisation scheme a signal to noise ratio for the calculated coefficients of 82 db. For a uniformly distributed white noise input this decreases to 75 db. We note that if the number of bits used in the quantiser is decreased the decrease in signal to noise ratio is 6 db per bit. The determination of the spectral distribution of the data was performed using an IBM370 computer and an I.M.S.L. library subroutine. It is not known what steps are provided in this routine to avoid overflow and to minimise roundoff errors in the computation but the 32 bit arithmetic capability of the computer would imply that the inherent limit on computational accuracy is the quantisation of the data which is only of 8 bits.

The residual frequency coefficients above 50 kHz (i.e. those components of the spectrum not considered to be generated by the detector scanning the image) obtained using the F.F.T. on real data are attributed to the noise in the signal processed with a minor contribution due to frequency smearing as a result of windowing of the data. A gaussian input pulse was used to test this result. With no quantisation of input data the ratio of residual coefficient amplitude to peak coefficient amplitude was found to be  $10^{-6}$ . When the data was truncated to 8 bits this increased to approximately  $3 \times 10^{-4}$  and with 7 bit quantisation this increased further to  $10^{-3}$ .

When the data was quantised to 6 bits the residual coefficients were found to be of the order of  $2 \times 10^{-3}$  times the peak coefficients. For data from AGA frames at sensitivities up to  $20^0$  the ratio is found to be of the order of  $2 \times 10^{-2}$  and the total signal to r.m.s. noise ratio is found to be of the order

of 40 to one which is consistent with observed noise on the lower sensitivity settings.

From these results and the Modulation Transfer Function of the AGA Thermovision it may then be assumed that under general conditions very little significant information is obtained from the field of view at spatial frequencies corresponding to video signal frequencies above 50 kHz. The noise input from the analogue to digital conversion process is less than that inherent in the AGA detector and electronics and the use of a 32 bit F.F.T. does not introduce significant errors in the determination of a spectral distribution. However it may be noted that if the dynamic range of the data is small with respect to the available 8 bit dynamic range of the analogue to digital converter the errors observed in the use of the data will increase accordingly since the effective number of quantisation levels decreases.

#### 4. ANALYSIS OF DATA

The AGA Thermovision does not allow the user to make any absolute determination of radiometric output and thus all measurements are made with respect to an 'effective' temperature difference. In use the instrument is calibrated using two black bodies at different temperatures (usually ambient and some temperature above ambient) and all measurements are then referred to this calibration.

By this means the user may determine the apparent emission in the 3.5  $\mu\text{m}$  to 5.5  $\mu\text{m}$  wavelength band (the AGA Thermovision response is not uniform across this band(ref.5) and hence any determination made must be made in accordance with this fact). Correction must also be made for atmospheric transmission effects if an estimate of actual emission from an object is to be made.

The AGA Thermovision then may be used as a scanning radiometer provided a number of error sources are accounted for. In general for extended sources (sources greater than 10 mrad in angular extent) the point values of the AGA video signal provide an estimate of the energy incident on the detector and the only corrections which need be applied are those for the atmospheric transmission effects and if possible the spectral sensitivity of the AGA. The integration of the radiance distribution over an extended source can be performed quite simply using the data acquisition system and performing the integration numerically. For extended sources the error in the integral will be negligible but in order to obtain a quantitative estimate of emission the instrument must be calibrated using an extended black body.

For sources of extent less than 10 mrad the errors due to signal compression caused by the detector field of view and the passband of the electronics must be accounted for if point estimates of emission are to be made. In estimating the total signal from a small source the integration limits must be chosen so as to minimise the errors due to the scanning process, and in estimating peak signal values from sampled data interpolation between adjacent sample values (in either sampling co-ordinate) should be performed using the sinc function reconstruction of the analogue waveform rather than linear interpolation. Numerical integration of the total signal may be performed for small sources with acceptable error limits (2 to 5 percent) if the integration limits are chosen using the criteria discussed previously and if the size of the source can be estimated.

Calibration is performed using two black bodies at known temperature positioned such that they both lie in the AGA field of view and thus can be observed together within a single frame. When scanning an object of radiance,  $N$ , the energy incident on the AGA detector is

$$H = N \cdot \Omega \cdot A \cdot t$$

where  $\Omega$  is the instantaneous field of view of the AGA,  $A$  is the collecting area of the optics and  $t$  is the atmospheric transmission. Thus the AGA signal can

be related to the target radiance distribution and the observed voltage is independent of the range of the target other than for the correction for transmission. The line scanning mechanism and the analogue to digital converter sample the target distribution every 0.9 mrad in the horizontal and vertical direction. Therefore if the observed signal difference between the two known black bodies is  $\Delta V_{\text{CAL}}$  for a radiance difference of  $\Delta N_{\text{CAL}}$  the emission from any other target distribution may be obtained as

$$H = 0.81 \times R^2 \times 10^{-6} \sum \frac{\Delta V \cdot \Delta N_{\text{CAL}}}{\Delta V_{\text{CAL}}} \text{ watt sr}^{-1}$$

where the summation is performed over the extent of the target distribution and the quantity  $0.81 \times R^2 \times 10^{-6}$  (where R is in cm) is the area subtended at the target by the sampling aperture (0.9 mrad square).

## 5. CONCLUSION

The use of a scanning (imaging) radiometer provides the ability to acquire large amounts of data on infrared emissions from objects and the use of digital processing techniques facilitates the analysis of more data than previously possible. However the data and processing may be subject to errors due to the nature of the scanning detector and the inherent limitations of digital (sampled) signal processing. In order to use the data adequately the user must be aware of these potential sources of error and correct for them. In particular for sources of less than 10 mrad extent accurate results must be dependent on good control of potential errors. This problem is of particular importance for the AGA Thermovision since with a field of view of only 70 mrad the potential for error in obtaining data using the system is quite high.

## REFERENCES

No.	Author	Title
1	Poropat, G.V.	"A Microprocessor Based Image Storage and Analysis Facility for Infrared Signature Measurement and Image Processing". DRCS Tech Memo ERL-0050-TM November 1978
2	Poropat, G.V.	"Determination of the Optimum Sampling Rate and Filter Parameters for Digital Processing of a Line Scanned Imaging System". WRE-TM-1559(AP) May 1976
3	Davis, D.J. and Rabinowitz, P.	"Numerical Integration". Blaisdell Publishing Company 1967
4	Oppenheim, A.V. and Schafer, R.W.	"Digital Signal Processing". Prentice Hall 1975
5	Rice, B.W.	"Infrared Measurements of a Murawa Sustainer Charge". WRE-TM-1917(A) December 1977

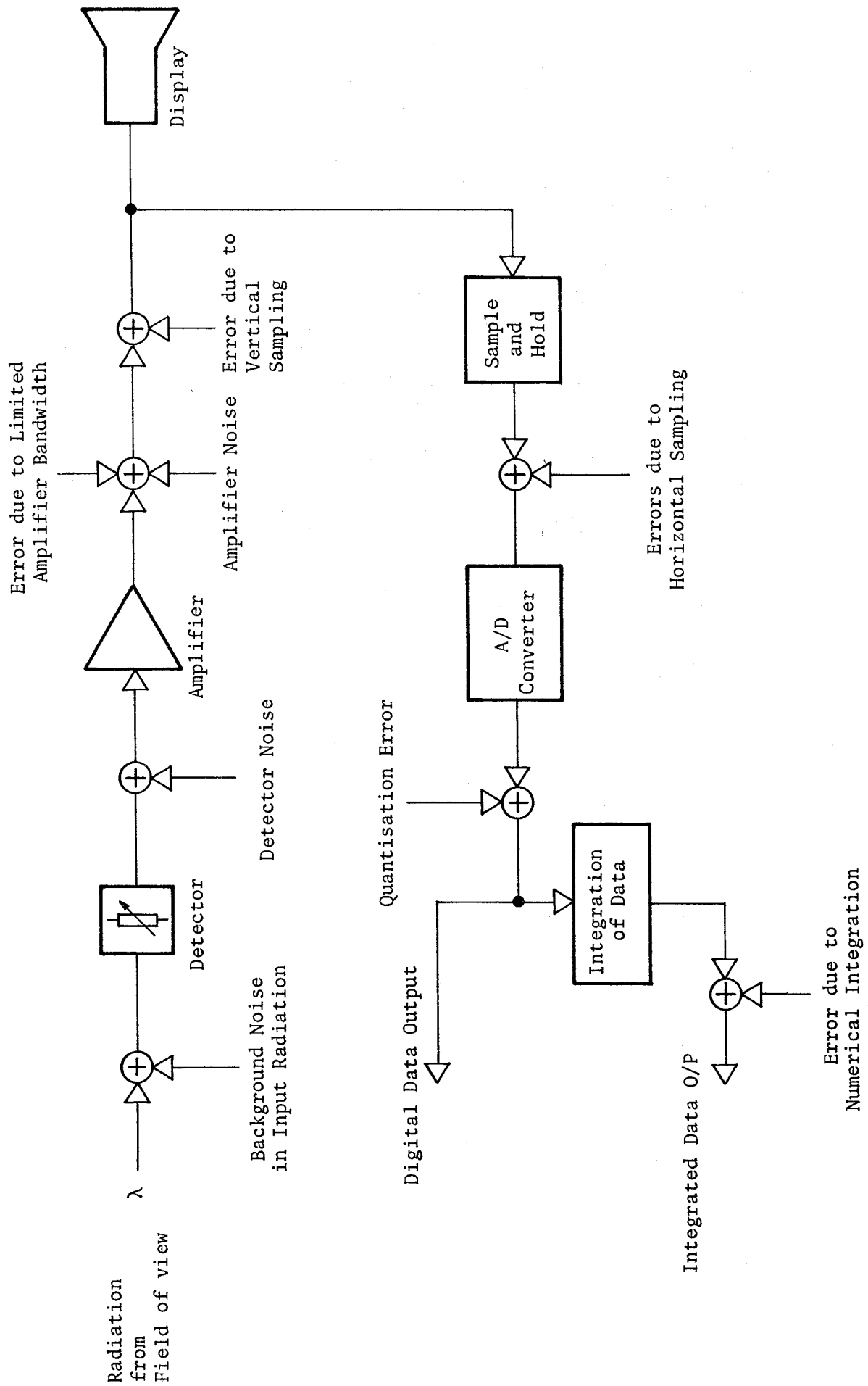


Figure 1. Signal flow graph for data acquisition and analysis

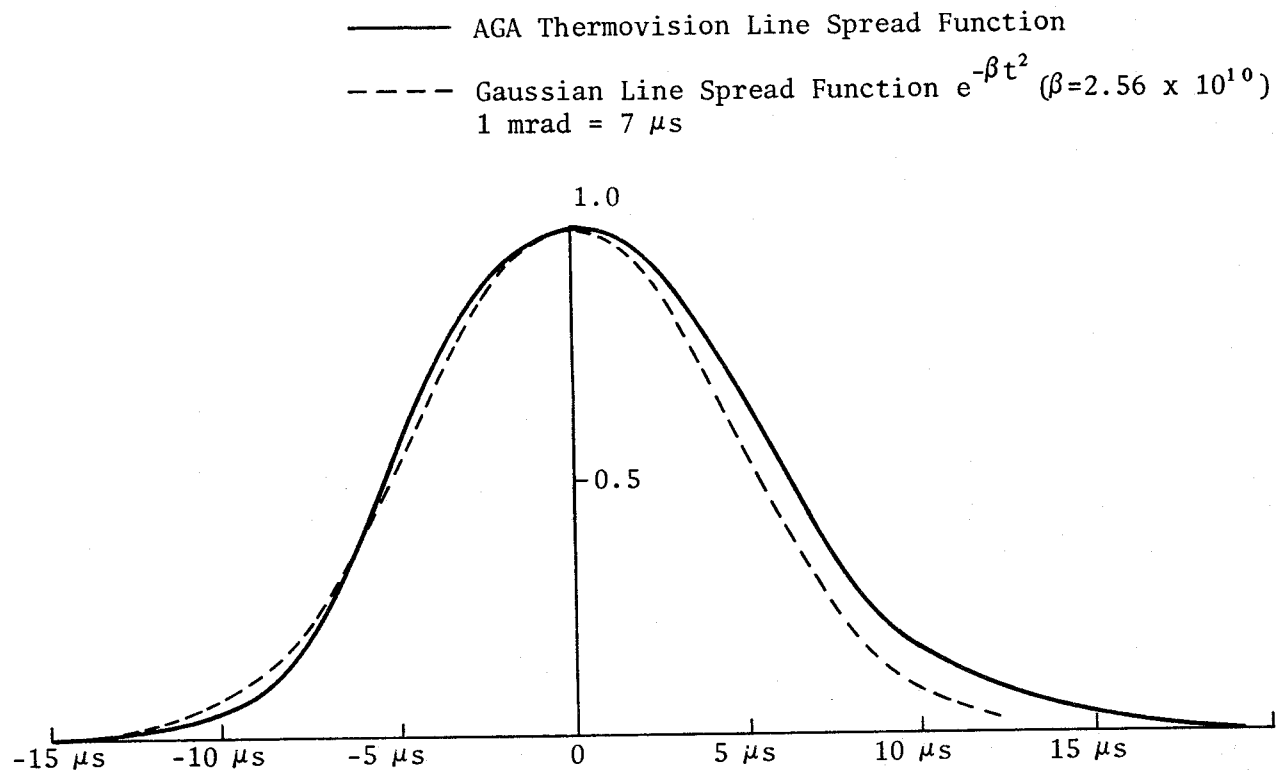


Figure 2. AGA Thermovision line spread function

- |                           |                            |
|---------------------------|----------------------------|
| 1 - Pulse Width 1 $\mu s$ | 5 - Pulse Width 8 $\mu s$  |
| 2 - Pulse Width 2 $\mu s$ | 6 - Pulse Width 10 $\mu s$ |
| 3 - Pulse Width 4 $\mu s$ | 7 - Pulse Width 20 $\mu s$ |
| 4 - Pulse Width 6 $\mu s$ | 8 - Pulse Width 30 $\mu s$ |

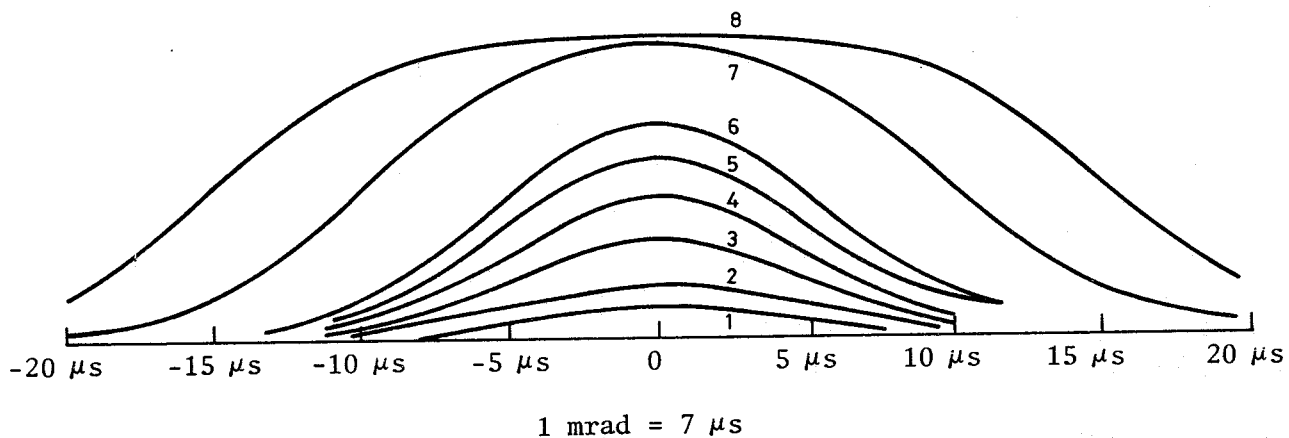


Figure 3. Pulse transfer function obtained using a gaussian line spread function



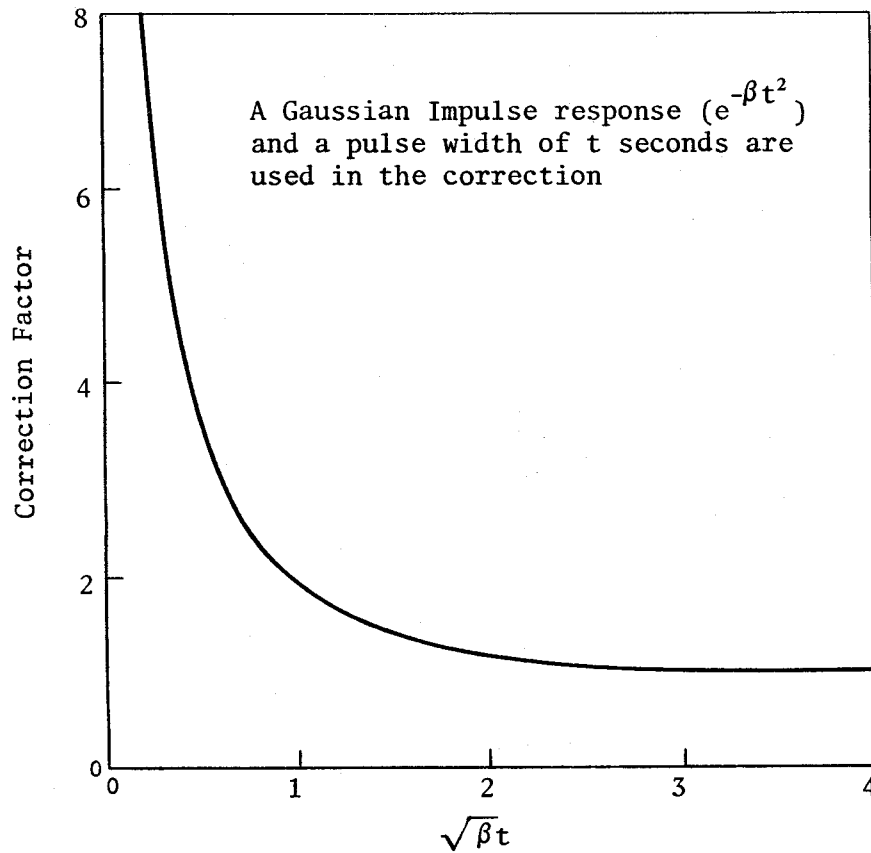


Figure 4. Pulse correction factor as a function of pulse width

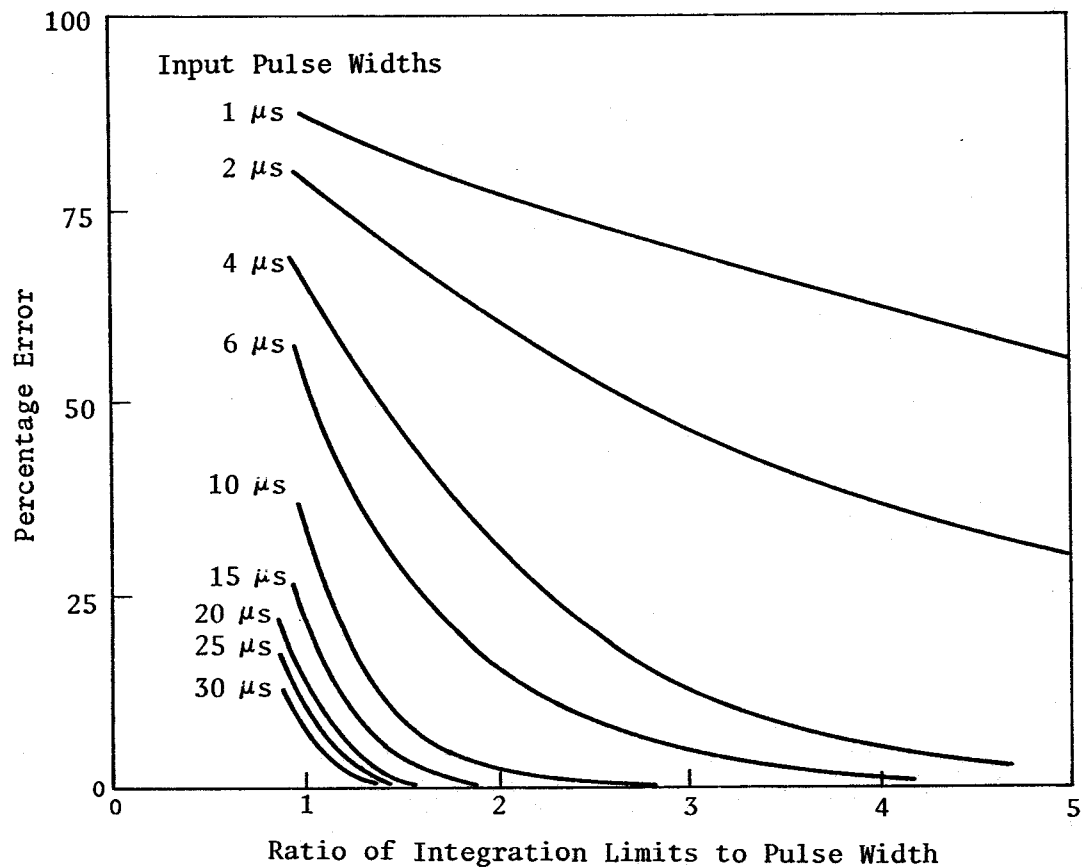


Figure 5. Variation of integral error with integration limits

## DOCUMENT CONTROL DATA SHEET

Security classification of this page

UNCLASSIFIED

1	DOCUMENT NUMBERS	2	SECURITY CLASSIFICATION
AR Number: AR-001-893		a. Complete Document: Unclassified	
Report Number: ERL-0099-TR		b. Title in Isolation: Unclassified	
Other Numbers:		c. Summary in Isolation: Unclassified	
3	TITLE		
RADIOMETRIC MEASUREMENTS USING LINE SCANNED INFRARED IMAGING SYSTEMS			
4	PERSONAL AUTHOR(S):	5	DOCUMENT DATE:
G.V. Poropat		August 1979	
6	6.1 TOTAL NUMBER OF PAGES 22		
6	6.2 NUMBER OF REFERENCES: 5		
7	7.1 CORPORATE AUTHOR(S):	8	REFERENCE NUMBERS
Electronics Research Laboratory		a. Task: DST 79/021	
7.2 DOCUMENT SERIES AND NUMBER Electronics Research Laboratory 0099-TR		b. Sponsoring Agency:	
9	COST CODE:		
308772			
10	IMPRINT (Publishing organisation)	11	COMPUTER PROGRAM(S) (Title(s) and language(s))
Defence Research Centre Salisbury			
12	RELEASE LIMITATIONS (of the document):		
Approved for Public Release			
12.0	OVERSEAS	NO	P.R. 1 A B C D E

Security classification of this page:

UNCLASSIFIED

## 13 ANNOUNCEMENT LIMITATIONS (of the information on these pages):

No limitation

## 14 DESCRIPTORS:

Infrared Equipment  
Radiometry  
Measuring instruments  
Radiation  
Data reduction

a. EJC Thesaurus  
Termsb. Non-Thesaurus  
Terms

Line scanned imaging  
Image processing

## 15 COSATI CODES:

1402

## 16 LIBRARY LOCATION CODES (for libraries listed in the distribution):

## 17 SUMMARY OR ABSTRACT:

(if this is security classified, the announcement of this report will be similarly classified)

The use of line scanned imaging systems in performing radiometric measurements enables the collection of considerable amounts of data which may be used in determining the distribution of radiant energy from a source. The interpretation of this data may be subject to errors due to the detector field of view and the scanning process. The sources of these errors and their magnitude are considered and guidelines for the analysis of the data developed.